

Search for Ultra-High-Energy Neutrinos at the Pierre Auger Observatory: New Triggers, Methods, and Constraints

Srijan Sehgal^{a,*} for the Pierre Auger Collaboration^b

^aBergische Universität Wuppertal, Wuppertal, Germany

^bObservatorio Pierre Auger, Av. San Martín Norte 304, 5613 Malargüe, Argentina

Full author list: https://www.auger.org/archive/authors_icrc_2025.html

E-mail: spokespersons@auger.org

The Pierre Auger Observatory has the capability to identify neutrino-induced extensive air showers above 10^{17} eV by using its large Surface Detector (SD) array. Data from the Observatory have been used to set some of the most stringent upper limits to the neutrino flux in the ultra-high energy (UHE) range. The data have also been used for follow-up detection of transient events in the context of multi-messenger astrophysics. In mid-2013, two additional SD triggers (Time-over-Threshold-deconvolved (ToTd) and Multiplicity-of-Positive Steps (MoPS)) were shown to increase the detection capability for the neutrino-induced air showers in the energy regime below 10^{19} eV by a factor of 5-10. This contribution will give an overview of the ongoing work regarding the searches for UHE neutrinos at the Pierre Auger Observatory. The impact of the ToTd and MoPS triggers for neutrino search in the zenith angle range of $60^\circ < \theta < 75^\circ$ is discussed. A novel neutrino identification method, which integrates these triggers, is applied to observational data to look for neutrino-like events using a *blind* search strategy. New constraints to point-like sources of UHE neutrinos will be presented for the angular range explored.

*Speaker

1. Introduction

Ultra-high-energy (UHE) neutrinos ($E > 10^{17}$ eV) are key to probing extreme astrophysical environments and understanding the origin of UHE cosmic rays (UHECRs) [1]. Unlike charged cosmic rays or high-energy photons, neutrinos travel vast distances unaffected by magnetic fields or significant attenuation, but their weak interactions make direct detection at UHE challenging. An effective method involves detecting extensive air showers (EAS) induced by neutrino charged-current (CC) or neutral-current (NC) interactions in the atmosphere or Earth, a technique employed by the Pierre Auger Observatory. Located in Argentina and covering 3000 km^2 , Pierre Auger Observatory combines a Surface Detector (SD) array of 1660 water-Cherenkov detectors (WCDs) with a Fluorescence Detector (FD) system comprising 27 fluorescence telescopes at four locations on its periphery.

The nearly continuous operation of the SD makes it well-suited for neutrino searches, having set one of the strongest limits on the diffuse UHE neutrino flux [2]. Neutrino-induced showers are classified as downward-going (DG) or Earth-skimming (ES), with DG further split into high and low zenith angles: DGH, $\theta \in [75^\circ, 90^\circ]$ and DGL $\theta \in [60^\circ, 75^\circ]$. This analysis focuses on the DGL range using SD data from 1st January 2014 up to 31st December 2021. A new selection incorporating all electromagnetic (EM) triggers is developed and tested on simulations, improving sensitivity to neutrino-induced EASs before being applied to data.

2. The electromagnetic triggers

The SD employs a hierarchical trigger system to identify air showers, starting from local station-level triggers up to array-wide and physics-level triggers [3]. Each WCD generates local triggers based on time-dependent signals, expressed in vertical equivalent muon (VEM) units, which corresponds to the total charge deposited by a single muon passing vertically through the water volume [3]. The initial triggers include the *threshold* (TH) trigger, optimized for muonic signals, and the *time-over-threshold* (ToT) trigger, more sensitive to EM components of an EAS. These are tuned to reject low-energy background, such as single muons and consequently pure EM signal.

To enhance sensitivity to EM-dominated showers, especially from neutrinos or photons, two additional triggers — *time-over-threshold-deconvolved* (ToTd) and *multiplicity-of-positive-steps* (MoPS) — were introduced in June 2013. ToTd compresses long exponential tail of diffusely reflected Cherenkov light associated with muon before applying a ToT condition to reduce background, while MoPS targets long non-smooth, low-amplitude signals typical of EM cascades. Both operate at a few Hz and are combined in a logical OR with ToT, effectively lowering the array’s energy threshold for detecting EM-rich air showers.

3. Search for UHE neutrinos $60^\circ < \theta < 75^\circ$

A key challenge in identifying UHE neutrino-induced EASs is distinguishing them from those initiated by UHECRs, such as protons or nuclei. The SD-based search at the Pierre Auger Observatory focuses on “young” showers — electromagnetic-rich and developing deep in the atmosphere—at zenith angles $\theta > 60^\circ$, where they contrast with “old,” muon-dominated CR

showers. Young showers produce broader, lower-peak SD signals, while old showers yield narrow, high-peak signals. At $\theta < 60^\circ$, this distinction blurs, limiting neutrino searches to more inclined geometries.

Selection relies on signal-based variables like the fraction of ToT triggers, tuned to broader signals [2]. Newer EM-sensitive triggers, ToTd and MoPS, further enhance sensitivity to low-energy (≤ 1 EeV) neutrinos by rejecting isolated muons. Another key variable is the Area-over-Peak (AoP), the ratio of the integrated signal to its peak, averaged over photo-multipliers; muon-like signals yield AoP values near 1, while EM signals show AoP > 1 .

3.1 Impact of ToTd and MoPS triggers

To evaluate the improvement in neutrino detection sensitivity from the addition of ToTd and MoPS triggers, simulated neutrino events reconstructed without these triggers were directly compared to the same events reconstructed with all triggers enabled. Figure 1 presents the total number of reconstructed events with and without ToTd and MoPS triggers across all energies and interaction channels (CC+ NC) as a function of the zenith angle.

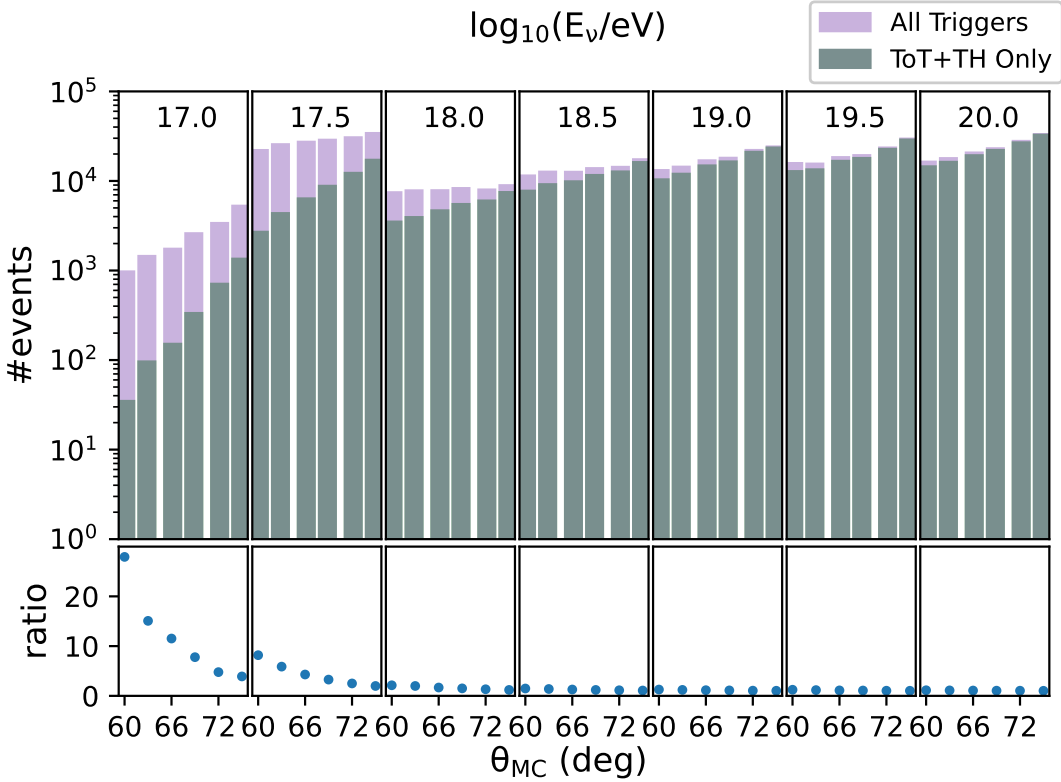


Figure 1: Reconstructed number of simulated neutrino events for all energies and channels (CC and NC) as a function of simulated zenith angle θ_{MC} for the sample with All (ToTd, MoPS + ToT, TH) triggers (purple bars) and only ToT+TH triggers (dark green bars). The bottom panel shows the ratio of the two samples.

The increase in reconstructed events is most pronounced at energies below ~ 1 EeV, largely due to the enhanced sensitivity of the ToTd and MoPS triggers to weaker, more electromagnetic-

dominated signals, which are characteristic of lower-energy neutrino-induced showers. This gain decreases at higher energies, where the *old* ToT and TH triggers already operate with high efficiency. Additionally, the effectiveness of ToTd and MoPS triggers varies with the zenith angle. At smaller zenith angles, neutrino showers retain a stronger electromagnetic component upon reaching the ground, making them more likely to be captured by ToTd and MoPS. At larger zenith angles, ToTd and MoPS triggers improve identification primarily for neutrinos that interact closer to the detector array, where the shower still contains an electromagnetic signature. Additionally, for shallower interaction points, the resulting showers become increasingly muonic due to atmospheric attenuation, reducing the added benefit of the ToTd and MoPS triggers. Although not explicitly shown, the overall gain in reconstructed events is notably greater for CC interactions than for NC ones. It was also observed that events reconstructed using all triggers typically have a larger multiplicity i.e. more stations enter in the reconstruction, increasing the possibility of the said event being selected as a neutrino candidate.

3.2 ν Selection

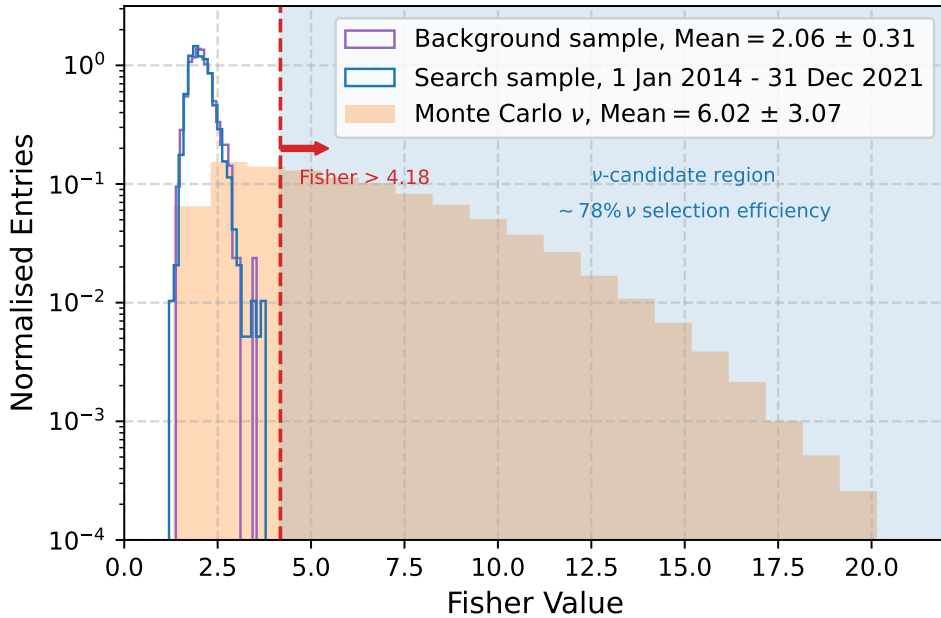


Figure 2: Distribution of the Fisher variable after the DGL event selection for events with reconstructed zenith angle $\theta_{\text{rec}} \in [67.5^\circ, 70.5^\circ]$. The open histograms show the background training sample (purple) and the search sample (blue) and the filled histogram (orange) depicts the simulated DGL ν events. Events above the Fisher value indicated by the vertical red dashed line would be regarded as neutrino candidates populating the blue-colored region.

Neutrino selection in the DGL range builds on the method in [2, 4], with refinements to include ToTd and MoPS triggers. Events must be fully contained within the SD, have a well-reconstructed zenith angle, and at least four triggered stations. A stricter EM condition is applied: 75% of stations closest to the core must have ToT, MoPS, or ToTd triggers to better reject background.

As in earlier work, Fisher Discriminant Analysis (FDA) [5] is used with five zenith sub-ranges to incorporate shower age. However, the discriminant now uses the sum of AoP values from the four earliest triggered stations near the core — shown via simulation to improve separation. The FDA is trained on 20% of the data selected at random from the analysis period to evaluate a detection threshold such that the expected background is fewer than one event in 20 years for the entire zenith angle range. Figure 2 shows the discriminant distribution for data and simulated ν -induced showers along with the evaluated cut in the $\theta_{\text{rec}} \in (67.5^\circ, 70.5^\circ]$ sub-range. Applying this selection, a search for neutrino-induced EASs was performed in the Observatory data between 1st January 2014 up to 31st December 2021. No neutrino candidates were found in any of the five DGL sub-regions.

4. Detector exposure and limits to the diffuse flux of UHE ν s in the DGL range

To use the non-observation of neutrino candidates for estimating an upper limit to the diffuse flux of UHE ν s in the DGL range, the exposure is estimated using MC simulations and the triangular shape of the SD grid. A hexagon is treated as the smallest effective detection unit for neutrino events, with a Brillouin effective area $A_{\text{hex}} = 1.95 \text{ km}^2$. The detector efficiency, $\varepsilon^{i,c}$ for a given hexagon depends on neutrino energy E_ν , interaction slant depth X , flavor i , interaction type c (CC or NC) and zenith angle θ , and the ground impact point of the air shower. Since the configuration of the SD array changes over time, the number of functional hexagons, $n_{\text{hex}}(t)$, recorded every minute, is used to model the evolution of the detector. The exposure $\xi^{i,c}(E_\nu)$ is then calculated by folding in the neutrino-nucleon cross-section $\sigma^{i,c}(E_\nu)$, the efficiency integrated over the parameter space (X, θ), and $n_{\text{hex}}(t)$, as shown in Eq. (1),

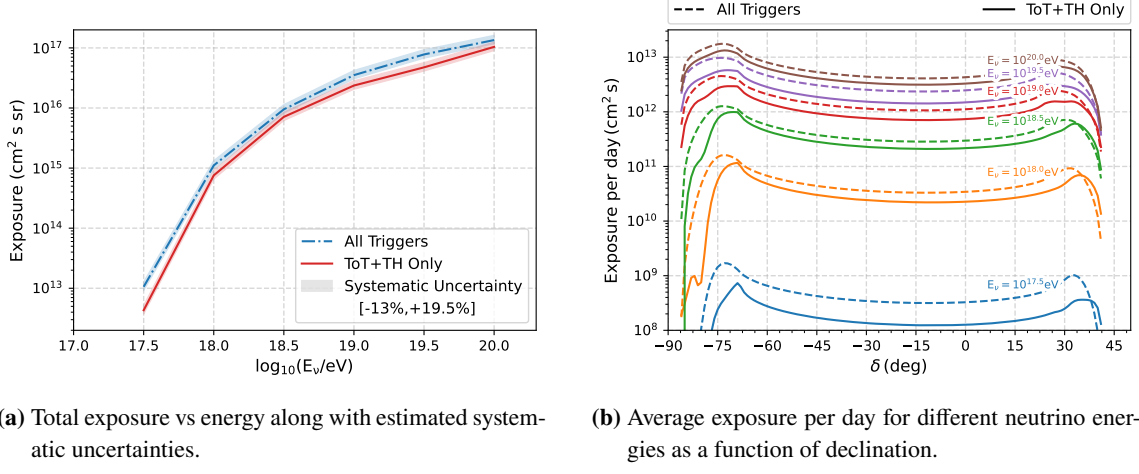
$$\xi^{i,c}(E_\nu) = \frac{\sigma^{i,c}(E_\nu)}{m_N} 2\pi \int_X \int_\theta \varepsilon^{i,c}(E_\nu, X, \theta) \sin \theta \cos \theta d\theta dX \int_t A_{\text{hex}} n_{\text{hex}}(t) dt. \quad (1)$$

The total integrated number of hexagons during the search period is $N_{\text{hex}} = 2.8 \times 10^{11} \text{ s}$, an equivalent of ~ 6.75 years of full-array operation. A total exposure, $\xi_{\text{tot}}(E_\nu) = \sum_i \sum_c \xi^{i,c}(E_\nu)$ is calculated by summing all the interaction channels and assuming a 1:1:1 flavour ratio at the earth, and is shown in Fig. 3a. The overall exposure benefits significantly from the addition of the new MoPS and ToTd triggers, particularly at lower energies (up to a 5 \times increase) especially in the ν_e CC channel, and from the improved FDA at higher energies. The electron neutrino CC interaction dominates the total exposure ($\sim 85\%$), while the NC contribution remains modest ($\sim 5\%$).

Assuming a power-law differential flux per unit area A , energy, solid angle Ω , and time of the form $\phi(E_\nu) = \frac{d^6 N_\nu}{dE_\nu d\Omega dA dt} = k \cdot E_\nu^{-2}$, an integrated upper limit on k is given by:

$$k_{90}^{\text{DGL}} = \frac{N_{90}}{\int_{E_\nu} E_\nu^{-2} \cdot \xi_{\text{tot}}(E_\nu) \cdot dE_\nu}, \quad (2)$$

where N_{90} is the upper limit on the number of expected signal events for zero background and a 90% confidence level. In this work, the Feldman–Cousins approach [6] extended to include systematic uncertainties [7, 8], is adopted yielding $N_{90} = 2.39$. The systematic uncertainties on exposure are $[-13\%, +19.5\%]$ taking into account the shortcomings of the neutrino simulations and their reconstruction, active hexagon counting and theoretical uncertainties associated with neutrino cross-section estimations at high energies.



(a) Total exposure vs energy along with estimated systematic uncertainties.

(b) Average exposure per day for different neutrino energies as a function of declination.

Figure 3: Comparisons of exposure to UHE ν in the DGL angular range for the time period 1 Jan 2014- 31 Dec 2021. The dashed lines are the exposures for this analysis, and the solid lines for the analysis performed with only ToT and TH triggers for the same time period.

The single flavour 90% C.L. integrated limit gives $k_{90}^{\text{DGL}} < 1.2 \times 10^{-7} \text{ GeV cm}^{-2}\text{s}^{-1}\text{sr}^{-1}$ in the DGL channel only. It applies to an energy range of $E_\nu \in [1.3 \times 10^{18} - 2.5 \times 10^{19.5}]$ in which $\sim 90\%$ of the total event rate is expected in the case of an E_ν^{-2} flux and is shown as a dashed purple line in Fig. 4. A *differential limit* can also be calculated by integrating the denominator of Eq. (2) in bins of width $\Delta = 0.5$ in $\log_{10}(E_\nu)$. The inclusion of ToTd and MoPS triggers leads to a 25% improvement of the estimated k_{90}^{DGL} . Although the DGL channel contributes little to the overall diffuse flux limit—still dominated by ES searches—it remains valuable for point-source studies due to its distinct field of view as discussed next.

5. Search for point-like sources of UHE ν s in the DGL range

Further, a dedicated search for point-like sources of UHE neutrinos using data collected in the DGL zenith angle range with the SD array of the Pierre Auger Observatory was also performed using the new ToTd and MoPS triggers. The method relies on the time-dependent visibility of candidate sources, which depends on the source declination δ and the corresponding zenith angle $\theta(t)$, expressed as $\cos \theta(t) = \sin \lambda \sin \delta + \cos \lambda \cos \delta \sin(2\pi t/T - \alpha)$, where λ is the latitude of the observatory and T is the duration of a sidereal day. A declination-dependent exposure $\xi(E_\nu, \delta)$ shown in Fig. 3b was calculated by estimating the time-dependent efficiencies and replacing them in Eq. (1). The exposure is largest for the declinations the source is seen the longest. The exposure is assumed to be uniform in right ascension within $\pm 0.6\%$ for the time period of search as shown in [9]. The non-detection of any neutrino candidates in the time period explored allowed us to set upper limits on the flux from point sources. Assuming a differential flux of the form $\phi(E_\nu) = k^{\text{PS}} E_\nu^{-2}$, the corresponding 90% confidence level upper limit on the normalization $k_{90}^{\text{PS,DGL}}$ is:

$$k_{90}^{\text{PS,DGL}} = \frac{N_{90}}{\int_{E_{\min}}^{E_{\max}} E_\nu^{-2} \xi(E_\nu, \delta) dE_\nu}. \quad (3)$$

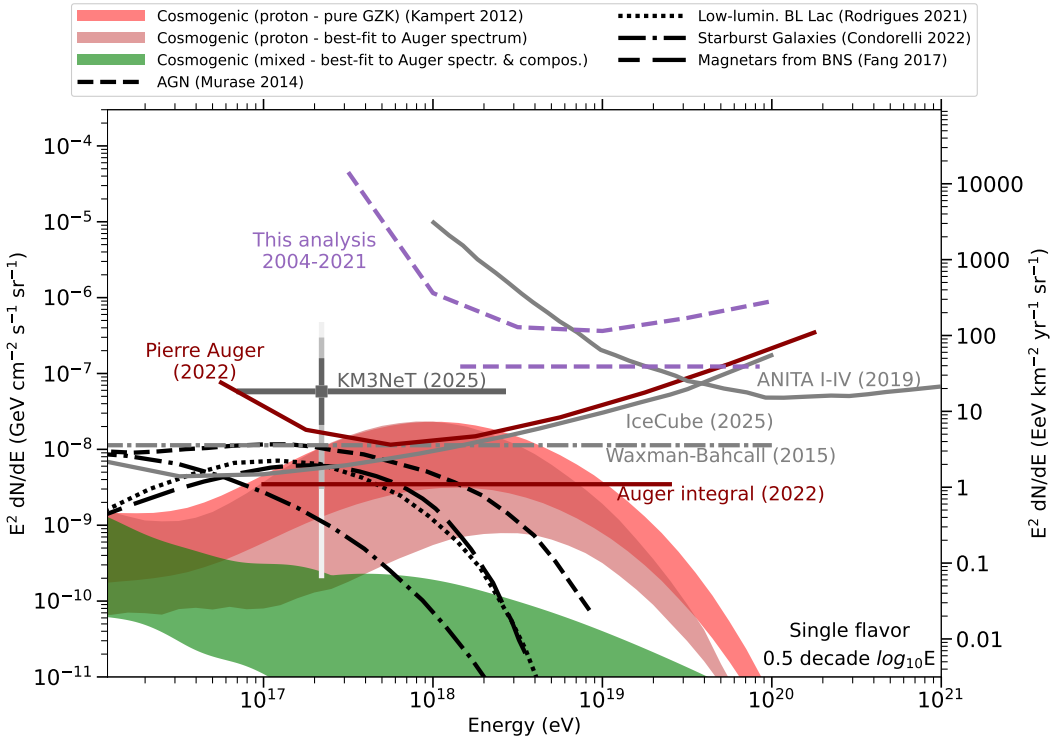


Figure 4: Comparison of the *limits* (1 Jan 2004-31 Dec 2013 with *ToT+TH* triggers and 1 Jan 2014-31 Dec 2021 with *All* triggers) to the current upper limits on the diffuse flux of UHE neutrinos. IceCube limits from [10] are scaled for a E_ν^{-2} flux assumption. The predicted fluxes from a few cosmogenic ν models are also shown.

Thanks to the improved EM triggers and updated discriminant methods, this analysis achieves a 1.5-fold improvement at the most sensitive declinations compared to the DGL analysis with only ToT and TH triggers. These results are contextualized within the broader zenith-angle neutrino search program at Auger, including comparisons with limits from the DGH and ES channels in Fig. 5. The inclusion of ToTd and MoPS triggers increases the neutrino detection efficiency at Auger between declinations $\delta \in (\approx -85^\circ, \approx 40^\circ)$, with a certain portion of the sky corresponding to $\delta \lesssim -68^\circ$ only visible in the DGL channel in comparison to other analyses.

6. Summary and Outlook

The Pierre Auger Observatory offers a large exposure to UHE neutrinos. The detector is continually improved to extend and enhance its detection capabilities. The analysis presented here quantifies one of these improvements by incorporating the triggers — Time-over-Threshold-deconvolved (ToTd) and Multiplicity-of-Positive-Steps (MoPS) — which were introduced to improve detection efficiency to small signals induced by the electromagnetic component of the shower. This analysis presents updated searches for UHEvs in the DGL zenith angle range $\theta \in [60^\circ, 75^\circ]$, incorporating all triggers. A novel selection built on an earlier analysis was introduced to search for neutrino candidates in 7 years of data. For the diffuse flux, the enhanced selection efficiency enabled a $\sim 25\%$ more stringent 90% C.L. upper limit, when compared to the previous selection, taking into

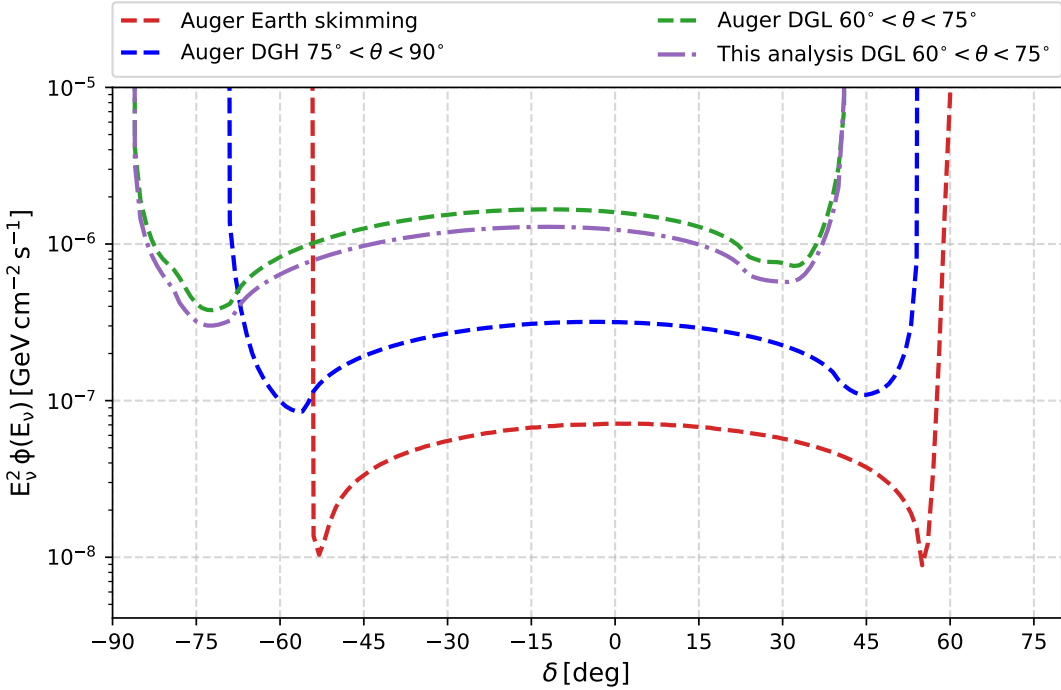


Figure 5: The upper limits (01.01.2004–31.12.2021) at 90% C.L. for different neutrino searches performed at the Pierre Auger Observatory of a single flavor point-like flux of UHE. The limit obtained in this analysis (purple) for the DGL channel is compared to the limits obtained for the DGH and ES channels [11].

account the DGL channel only. In point-source searches, improved detection efficiency led to increased directional exposure and stricter declination-dependent upper limits. Although the absolute gains in sensitivity obtained in this work are relatively modest, and the Pierre Auger limit is still dominated by the Earth-Skimming channel, they are crucial, especially in the $E_\nu \gtrsim 10^{18}$ eV regime and especially in declinations $\delta \lesssim -68^\circ$ exclusively accessible in DGL. These results underline the scientific value of leveraging ToTd and MoPS triggered data and motivate further refinements to reconstruction algorithms for future UHE neutrino searches.

References

- [1] A. Coleman et al., *Astropart. Phys.* **149** (2023) 102819 [[arXiv:2205.05845](#)].
- [2] A. Aab et al. [Pierre Auger Coll.], *JCAP* **10** (2019) 022 [[arXiv:1906.07422](#)].
- [3] J. Abraham et al. [Pierre Auger Coll.], *Nucl. Instrum. Meth. A* **613** (2022) 29–39 [[arXiv:1111.6764](#)].
- [4] J. L. Navarro Quirante, *Thesis Univ. Granada* (2013).
- [5] R. A. Fisher, *Annals Eugen.* **7** (1936) 179–188.
- [6] G. J. Feldman and R. D. Cousins, *Phys. Rev. D* **57** (1998) 3873–3889 [[arXiv:physics/9711021](#)].
- [7] A. Aab et al. [Pierre Auger Coll.], *Phys. Rev. D* **91** (9) (2015) 092008 [[arXiv:1504.05397](#)].
- [8] J. Conrad, et al., *Phys. Rev. D* **67** (2003) 092008 [[arXiv:hep-ex/0202013](#)].
- [9] A. Aab et al. [Pierre Auger Coll.], *Science* **357** (6537) (2017) 1266–1270 [[arXiv:1709.07321](#)].
- [10] R. Abbasi et al. [IceCube Coll.], [[arXiv:2502.01963](#)].
- [11] A. Aab et al. [Pierre Auger Coll.], *JCAP* **11** (2019) 004 [[arXiv:1906.07419](#)].

The Pierre Auger Collaboration



PIERRE
AUGER
OBSERVATORY

- A. Abdul Halim¹³, P. Abreu⁷⁰, M. Aglietta^{53,51}, I. Allekotte¹, K. Almeida Cheminant^{78,77}, A. Almela^{7,12}, R. Aloisio^{44,45}, J. Alvarez-Muñiz⁷⁶, A. Ambrosone⁴⁴, J. Ammerman Yebra⁷⁶, G.A. Anastasi^{57,46}, L. Anchordoqui⁸³, B. Andrade⁷, L. Andrade Dourado^{44,45}, S. Andringa⁷⁰, L. Apollonio^{58,48}, C. Aramo⁴⁹, E. Arnone^{62,51}, J.C. Arteaga Velázquez⁶⁶, P. Assis⁷⁰, G. Avila¹¹, E. Avocone^{56,45}, A. Bakalova³¹, F. Barbato^{44,45}, A. Bartz Mocellin⁸², J.A. Bellido¹³, C. Berat³⁵, M.E. Bertaina^{62,51}, M. Bianciotto^{62,51}, P.L. Biermann^a, V. Binet⁵, K. Bismarck^{38,7}, T. Bister^{77,78}, J. Biteau^{36,i}, J. Blazek³¹, J. Blümmer⁴⁰, M. Boháčová³¹, D. Boncioli^{56,45}, C. Bonifazi⁸, L. Bonneau Arbeletche²², N. Borodai⁶⁸, J. Brack^f, P.G. Brichetto Orchera^{7,40}, F.L. Briechle⁴¹, A. Bueno⁷⁵, S. Buitink¹⁵, M. Buscemi^{46,57}, M. Büsken^{38,7}, A. Bwembya^{77,78}, K.S. Caballero-Mora⁶⁵, S. Cabana-Freire⁷⁶, L. Caccianiga^{58,48}, F. Campuzano⁶, J. Caraça-Valente⁸², R. Caruso^{57,46}, A. Castellina^{53,51}, F. Catalani¹⁹, G. Cataldi⁴⁷, L. Cazon⁷⁶, M. Cerda¹⁰, B. Čermáková⁴⁰, A. Cermenati^{44,45}, J.A. Chinellato²², J. Chudoba³¹, L. Chytka³², R.W. Clay¹³, A.C. Cobos Cerutti⁶, R. Colalillo^{59,49}, R. Conceição⁷⁰, G. Consolati^{48,54}, M. Conte^{55,47}, F. Convenga^{44,45}, D. Correia dos Santos²⁷, P.J. Costa⁷⁰, C.E. Covault⁸¹, M. Cristinziani⁴³, C.S. Cruz Sanchez³, S. Dasso^{4,2}, K. Daumiller⁴⁰, B.R. Dawson¹³, R.M. de Almeida²⁷, E.-T. de Boone⁴³, B. de Errico²⁷, J. de Jesús⁷, S.J. de Jong^{77,78}, J.R.T. de Mello Neto²⁷, I. De Mitri^{44,45}, J. de Oliveira¹⁸, D. de Oliveira Franco⁴², F. de Palma^{55,47}, V. de Souza²⁰, E. De Vito^{55,47}, A. Del Popolo^{57,46}, O. Deligny³³, N. Denner³¹, L. Deval^{53,51}, A. di Matteo⁵¹, C. Dobrigkeit²², J.C. D'Olivo⁶⁷, L.M. Domingues Mendes^{16,70}, Q. Dorosti⁴³, J.C. dos Anjos¹⁶, R.C. dos Anjos²⁶, J. Ebr³¹, F. Ellwanger⁴⁰, R. Engel^{38,40}, I. Epicoco^{55,47}, M. Erdmann⁴¹, A. Etchegoyen^{7,12}, C. Evoli^{44,45}, H. Falcke^{77,79,78}, G. Farrar⁸⁵, A.C. Fauth²², T. Fehler⁴³, F. Feldbusch³⁹, A. Fernandes⁷⁰, M. Fernandez¹⁴, B. Fick⁸⁴, J.M. Figueira⁷, P. Filip^{38,7}, A. Filipčič^{74,73}, T. Fitoussi⁴⁰, B. Flaggs⁸⁷, T. Fodran⁷⁷, A. Franco⁴⁷, M. Freitas⁷⁰, T. Fujii^{86,h}, A. Fuster^{7,12}, C. Galea⁷⁷, B. García⁶, C. Gaudu³⁷, P.L. Ghia³³, U. Giaccari⁴⁷, F. Gobbi¹⁰, F. Gollan⁷, G. Golup¹, M. Gómez Berisso¹, P.F. Gómez Vitale¹¹, J.P. Gongora¹¹, J.M. González¹, N. González⁷, D. Góra⁶⁸, A. Gorgi^{53,51}, M. Gottowik⁴⁰, F. Guarino^{59,49}, G.P. Guedes²³, L. Gültzow⁴⁰, S. Hahn³⁸, P. Hamal³¹, M.R. Hampel⁷, P. Hansen³, V.M. Harvey¹³, A. Haungs⁴⁰, T. Hebbeker⁴¹, C. Hojvat^d, J.R. Hörandel^{77,78}, P. Horvath³², M. Hrabovský³², T. Huege^{40,15}, A. Insolia^{57,46}, P.G. Isar⁷², M. Ismaiel^{77,78}, P. Janecek³¹, V. Jilek³¹, K.-H. Kampert³⁷, B. Keilhauer⁴⁰, A. Khakurdikar⁷⁷, V.V. Kizakke Covilakam^{7,40}, H.O. Klages⁴⁰, M. Kleifges³⁹, J. Köhler⁴⁰, F. Krieger⁴¹, M. Kubatova³¹, N. Kunka³⁹, B.L. Lago¹⁷, N. Langner⁴¹, N. Leal⁷, M.A. Leigui de Oliveira²⁵, Y. Lema-Capeans⁷⁶, A. Letessier-Selvon³⁴, I. Lhenry-Yvon³³, L. Lopes⁷⁰, J.P. Lundquist⁷³, M. Mallamaci^{60,46}, D. Mandat³¹, P. Mantsch^d, F.M. Marianj^{58,48}, A.G. Mariazzi³, I.C. Mariş¹⁴, G. Marsella^{60,46}, D. Martello^{55,47}, S. Martinelli^{40,7}, M.A. Martins⁷⁶, H.-J. Mathes⁴⁰, J. Matthews^g, G. Matthiae^{61,50}, E. Mayotte⁸², S. Mayotte⁸², P.O. Mazur^d, G. Medina-Tanco⁶⁷, J. Meinert³⁷, D. Melo⁷, A. Menshikov³⁹, C. Merx⁴⁰, S. Michal³¹, M.I. Micheletti⁵, L. Miramonti^{58,48}, M. Mogarkar⁶⁸, S. Mollerach¹, F. Montanet³⁵, L. Morejon³⁷, K. Mulrey^{77,78}, R. Mussa⁵¹, W.M. Namasaka³⁷, S. Negi³¹, L. Nellen⁶⁷, K. Nguyen⁸⁴, G. Nicora⁹, M. Niechciol⁴³, D. Nitz⁸⁴, D. Nosek³⁰, A. Novikov⁸⁷, V. Novotny³⁰, L. Nožka³², A. Nucita^{55,47}, L.A. Núñez²⁹, J. Ochoa^{7,40}, C. Oliveira²⁰, L. Östman³¹, M. Palatka³¹, J. Pallotta⁹, S. Panja³¹, G. Parente⁷⁶, T. Paulsen³⁷, J. Pawlowsky³⁷, M. Pech³¹, J. Pękala⁶⁸, R. Pelayo⁶⁴, V. Pelgrims¹⁴, L.A.S. Pereira²⁴, E.E. Pereira Martins^{38,7}, C. Pérez Bertolli^{7,40}, L. Perrone^{55,47}, S. Petrera^{44,45}, C. Petrucci⁵⁶, T. Pierog⁴⁰, M. Pimenta⁷⁰, M. Platino⁷, B. Pont⁷⁷, M. Pour-mohammad Shahvar^{60,46}, P. Privitera⁸⁶, C. Priyatadarshi⁶⁸, M. Prouza³¹, K. Pytel⁶⁹, S. Querchfeld³⁷, J. Rautenberg³⁷, D. Ravignani⁷, J.V. Reginatto Akim²², A. Reuzki⁴¹, J. Ridky³¹, F. Riehn^{76,j}, M. Risse⁴³, V. Rizi^{56,45}, E. Rodriguez^{7,40}, G. Rodriguez Fernandez⁵⁰, J. Rodriguez Rojo¹¹, S. Rossoni⁴², M. Roth⁴⁰, E. Roulet¹, A.C. Rovero⁴, A. Saftoiu⁷¹, M. Saharan⁷⁷, F. Salamida^{56,45}, H. Salazar⁶³, G. Salina⁵⁰, P. Sampathkumar⁴⁰, N. San Martin⁸², J.D. Sanabria Gomez²⁹, F. Sánchez⁷, E.M. Santos²¹, E. Santos³¹, F. Sarazin⁸², R. Sarmento⁷⁰, R. Sato¹¹, P. Savina^{44,45}, V. Scherini^{55,47}, H. Schieler⁴⁰, M. Schimassek³³, M. Schimp³⁷, D. Schmidt⁴⁰, O. Scholten^{15,b}, H. Schoorlemmer^{77,78}, P. Schovánek³¹, F.G. Schröder^{87,40},

J. Schulte⁴¹, T. Schulz³¹, S.J. Sciutto³, M. Scornavacche⁷, A. Sedoski⁷, A. Segreto^{52,46}, S. Sehgal³⁷, S.U. Shivashankara⁷³, G. Sigl⁴², K. Simkova^{15,14}, F. Simon³⁹, R. Šmídá⁸⁶, P. Sommers^e, R. Squartini¹⁰, M. Stadelmaier^{40,48,58}, S. Stanic⁷³, J. Stasielak⁶⁸, P. Stassi³⁵, S. Strähnz³⁸, M. Straub⁴¹, T. Suomijärvi³⁶, A.D. Supanitsky⁷, Z. Svozilíkova³¹, K. Syrokvas³⁰, Z. Szadkowski⁶⁹, F. Tairli¹³, M. Tambone^{59,49}, A. Tapia²⁸, C. Taricco^{62,51}, C. Timmermans^{78,77}, O. Tkachenko³¹, P. Tobiska³¹, C.J. Todero Peixoto¹⁹, B. Tomé⁷⁰, A. Travaini¹⁰, P. Travnicek³¹, M. Tueros³, M. Unger⁴⁰, R. Uzeiroska³⁷, L. Vaclavek³², M. Vacula³², I. Vaiman^{44,45}, J.F. Valdés Galicia⁶⁷, L. Valore^{59,49}, P. van Dillen^{77,78}, E. Varela⁶³, V. Vašíčková³⁷, A. Vásquez-Ramírez²⁹, D. Veberič⁴⁰, I.D. Vergara Quispe³, S. Verpoest⁸⁷, V. Verzi⁵⁰, J. Vicha³¹, J. Vink⁸⁰, S. Vorobiov⁷³, J.B. Vuta³¹, C. Watanabe²⁷, A.A. Watson^c, A. Weindl⁴⁰, M. Weitz³⁷, L. Wiencke⁸², H. Wilczyński⁶⁸, B. Wundheiler⁷, B. Yue³⁷, A. Yushkov³¹, E. Zas⁷⁶, D. Zavrtanik^{73,74}, M. Zavrtanik^{74,73}

¹ Centro Atómico Bariloche and Instituto Balseiro (CNEA-UNCuyo-CONICET), San Carlos de Bariloche, Argentina

² Departamento de Física and Departamento de Ciencias de la Atmósfera y los Océanos, FCEyN, Universidad de Buenos Aires and CONICET, Buenos Aires, Argentina

³ IFLP, Universidad Nacional de La Plata and CONICET, La Plata, Argentina

⁴ Instituto de Astronomía y Física del Espacio (IAFE, CONICET-UBA), Buenos Aires, Argentina

⁵ Instituto de Física de Rosario (IFIR) – CONICET/U.N.R. and Facultad de Ciencias Bioquímicas y Farmacéuticas U.N.R., Rosario, Argentina

⁶ Instituto de Tecnologías en Detección y Astropartículas (CNEA, CONICET, UNSAM), and Universidad Tecnológica Nacional – Facultad Regional Mendoza (CONICET/CNEA), Mendoza, Argentina

⁷ Instituto de Tecnologías en Detección y Astropartículas (CNEA, CONICET, UNSAM), Buenos Aires, Argentina

⁸ International Center of Advanced Studies and Instituto de Ciencias Físicas, ECyT-UNSAM and CONICET, Campus Miguelete – San Martín, Buenos Aires, Argentina

⁹ Laboratorio Atmósfera – Departamento de Investigaciones en Láseres y sus Aplicaciones – UNIDEF (CITEDEF-CONICET), Argentina

¹⁰ Observatorio Pierre Auger, Malargüe, Argentina

¹¹ Observatorio Pierre Auger and Comisión Nacional de Energía Atómica, Malargüe, Argentina

¹² Universidad Tecnológica Nacional – Facultad Regional Buenos Aires, Buenos Aires, Argentina

¹³ University of Adelaide, Adelaide, S.A., Australia

¹⁴ Université Libre de Bruxelles (ULB), Brussels, Belgium

¹⁵ Vrije Universiteit Brussels, Brussels, Belgium

¹⁶ Centro Brasileiro de Pesquisas Fisicas, Rio de Janeiro, RJ, Brazil

¹⁷ Centro Federal de Educação Tecnológica Celso Suckow da Fonseca, Petropolis, Brazil

¹⁸ Instituto Federal de Educação, Ciência e Tecnologia do Rio de Janeiro (IFRJ), Brazil

¹⁹ Universidade de São Paulo, Escola de Engenharia de Lorena, Lorena, SP, Brazil

²⁰ Universidade de São Paulo, Instituto de Física de São Carlos, São Carlos, SP, Brazil

²¹ Universidade de São Paulo, Instituto de Física, São Paulo, SP, Brazil

²² Universidade Estadual de Campinas (UNICAMP), IFGW, Campinas, SP, Brazil

²³ Universidade Estadual de Feira de Santana, Feira de Santana, Brazil

²⁴ Universidade Federal de Campina Grande, Centro de Ciencias e Tecnologia, Campina Grande, Brazil

²⁵ Universidade Federal do ABC, Santo André, SP, Brazil

²⁶ Universidade Federal do Paraná, Setor Palotina, Palotina, Brazil

²⁷ Universidade Federal do Rio de Janeiro, Instituto de Física, Rio de Janeiro, RJ, Brazil

²⁸ Universidad de Medellín, Medellín, Colombia

²⁹ Universidad Industrial de Santander, Bucaramanga, Colombia

³⁰ Charles University, Faculty of Mathematics and Physics, Institute of Particle and Nuclear Physics, Prague, Czech Republic

³¹ Institute of Physics of the Czech Academy of Sciences, Prague, Czech Republic

³² Palacky University, Olomouc, Czech Republic

³³ CNRS/IN2P3, IJCLab, Université Paris-Saclay, Orsay, France

- ³⁴ Laboratoire de Physique Nucléaire et de Hautes Energies (LPNHE), Sorbonne Université, Université de Paris, CNRS-IN2P3, Paris, France
- ³⁵ Univ. Grenoble Alpes, CNRS, Grenoble Institute of Engineering Univ. Grenoble Alpes, LPSC-IN2P3, 38000 Grenoble, France
- ³⁶ Université Paris-Saclay, CNRS/IN2P3, IJCLab, Orsay, France
- ³⁷ Bergische Universität Wuppertal, Department of Physics, Wuppertal, Germany
- ³⁸ Karlsruhe Institute of Technology (KIT), Institute for Experimental Particle Physics, Karlsruhe, Germany
- ³⁹ Karlsruhe Institute of Technology (KIT), Institut für Prozessdatenverarbeitung und Elektronik, Karlsruhe, Germany
- ⁴⁰ Karlsruhe Institute of Technology (KIT), Institute for Astroparticle Physics, Karlsruhe, Germany
- ⁴¹ RWTH Aachen University, III. Physikalisches Institut A, Aachen, Germany
- ⁴² Universität Hamburg, II. Institut für Theoretische Physik, Hamburg, Germany
- ⁴³ Universität Siegen, Department Physik – Experimentelle Teilchenphysik, Siegen, Germany
- ⁴⁴ Gran Sasso Science Institute, L'Aquila, Italy
- ⁴⁵ INFN Laboratori Nazionali del Gran Sasso, Assergi (L'Aquila), Italy
- ⁴⁶ INFN, Sezione di Catania, Catania, Italy
- ⁴⁷ INFN, Sezione di Lecce, Lecce, Italy
- ⁴⁸ INFN, Sezione di Milano, Milano, Italy
- ⁴⁹ INFN, Sezione di Napoli, Napoli, Italy
- ⁵⁰ INFN, Sezione di Roma “Tor Vergata”, Roma, Italy
- ⁵¹ INFN, Sezione di Torino, Torino, Italy
- ⁵² Istituto di Astrofisica Spaziale e Fisica Cosmica di Palermo (INAF), Palermo, Italy
- ⁵³ Osservatorio Astrofisico di Torino (INAF), Torino, Italy
- ⁵⁴ Politecnico di Milano, Dipartimento di Scienze e Tecnologie Aerospaziali , Milano, Italy
- ⁵⁵ Università del Salento, Dipartimento di Matematica e Fisica “E. De Giorgi”, Lecce, Italy
- ⁵⁶ Università dell’Aquila, Dipartimento di Scienze Fisiche e Chimiche, L’Aquila, Italy
- ⁵⁷ Università di Catania, Dipartimento di Fisica e Astronomia “Ettore Majorana“, Catania, Italy
- ⁵⁸ Università di Milano, Dipartimento di Fisica, Milano, Italy
- ⁵⁹ Università di Napoli “Federico II”, Dipartimento di Fisica “Ettore Pancini”, Napoli, Italy
- ⁶⁰ Università di Palermo, Dipartimento di Fisica e Chimica ”E. Segrè”, Palermo, Italy
- ⁶¹ Università di Roma “Tor Vergata”, Dipartimento di Fisica, Roma, Italy
- ⁶² Università Torino, Dipartimento di Fisica, Torino, Italy
- ⁶³ Benemérita Universidad Autónoma de Puebla, Puebla, México
- ⁶⁴ Unidad Profesional Interdisciplinaria en Ingeniería y Tecnologías Avanzadas del Instituto Politécnico Nacional (UPIITA-IPN), México, D.F., México
- ⁶⁵ Universidad Autónoma de Chiapas, Tuxtla Gutiérrez, Chiapas, México
- ⁶⁶ Universidad Michoacana de San Nicolás de Hidalgo, Morelia, Michoacán, México
- ⁶⁷ Universidad Nacional Autónoma de México, México, D.F., México
- ⁶⁸ Institute of Nuclear Physics PAN, Krakow, Poland
- ⁶⁹ University of Łódź, Faculty of High-Energy Astrophysics, Łódź, Poland
- ⁷⁰ Laboratório de Instrumentação e Física Experimental de Partículas – LIP and Instituto Superior Técnico – IST, Universidade de Lisboa – UL, Lisboa, Portugal
- ⁷¹ “Horia Hulubei” National Institute for Physics and Nuclear Engineering, Bucharest-Magurele, Romania
- ⁷² Institute of Space Science, Bucharest-Magurele, Romania
- ⁷³ Center for Astrophysics and Cosmology (CAC), University of Nova Gorica, Nova Gorica, Slovenia
- ⁷⁴ Experimental Particle Physics Department, J. Stefan Institute, Ljubljana, Slovenia
- ⁷⁵ Universidad de Granada and C.A.F.P.E., Granada, Spain
- ⁷⁶ Instituto Galego de Física de Altas Enerxías (IGFAE), Universidade de Santiago de Compostela, Santiago de Compostela, Spain
- ⁷⁷ IMAPP, Radboud University Nijmegen, Nijmegen, The Netherlands
- ⁷⁸ Nationaal Instituut voor Kernfysica en Hoge Energie Fysica (NIKHEF), Science Park, Amsterdam, The Netherlands
- ⁷⁹ Stichting Astronomisch Onderzoek in Nederland (ASTRON), Dwingeloo, The Netherlands
- ⁸⁰ Universiteit van Amsterdam, Faculty of Science, Amsterdam, The Netherlands

⁸¹ Case Western Reserve University, Cleveland, OH, USA

⁸² Colorado School of Mines, Golden, CO, USA

⁸³ Department of Physics and Astronomy, Lehman College, City University of New York, Bronx, NY, USA

⁸⁴ Michigan Technological University, Houghton, MI, USA

⁸⁵ New York University, New York, NY, USA

⁸⁶ University of Chicago, Enrico Fermi Institute, Chicago, IL, USA

⁸⁷ University of Delaware, Department of Physics and Astronomy, Bartol Research Institute, Newark, DE, USA

^a Max-Planck-Institut für Radioastronomie, Bonn, Germany

^b also at Kapteyn Institute, University of Groningen, Groningen, The Netherlands

^c School of Physics and Astronomy, University of Leeds, Leeds, United Kingdom

^d Fermi National Accelerator Laboratory, Fermilab, Batavia, IL, USA

^e Pennsylvania State University, University Park, PA, USA

^f Colorado State University, Fort Collins, CO, USA

^g Louisiana State University, Baton Rouge, LA, USA

^h now at Graduate School of Science, Osaka Metropolitan University, Osaka, Japan

ⁱ Institut universitaire de France (IUF), France

^j now at Technische Universität Dortmund and Ruhr-Universität Bochum, Dortmund and Bochum, Germany

Acknowledgments

The successful installation, commissioning, and operation of the Pierre Auger Observatory would not have been possible without the strong commitment and effort from the technical and administrative staff in Malargüe. We are very grateful to the following agencies and organizations for financial support:

Argentina – Comisión Nacional de Energía Atómica; Agencia Nacional de Promoción Científica y Tecnológica (ANPCyT); Consejo Nacional de Investigaciones Científicas y Técnicas (CONICET); Gobierno de la Provincia de Mendoza; Municipalidad de Malargüe; NDM Holdings and Valle Las Leñas; in gratitude for their continuing cooperation over land access; Australia – the Australian Research Council; Belgium – Fonds de la Recherche Scientifique (FNRS); Research Foundation Flanders (FWO), Marie Curie Action of the European Union Grant No. 101107047; Brazil – Conselho Nacional de Desenvolvimento Científico e Tecnológico (CNPq); Financiadora de Estudos e Projetos (FINEP); Fundação de Amparo à Pesquisa do Estado de Rio de Janeiro (FAPERJ); São Paulo Research Foundation (FAPESP) Grants No. 2019/10151-2, No. 2010/07359-6 and No. 1999/05404-3; Ministério da Ciência, Tecnologia, Inovações e Comunicações (MCTIC); Czech Republic – GACR 24-13049S, CAS LQ100102401, MEYS LM2023032, CZ.02.1.01/0.0/0.0/16_013/0001402, CZ.02.1.01/0.0/0.0/18_046/0016010 and CZ.02.1.01/0.0/0.0/17_049/0008422 and CZ.02.01.01/00/22_008/0004632; France – Centre de Calcul IN2P3/CNRS; Centre National de la Recherche Scientifique (CNRS); Conseil Régional Ile-de-France; Département Physique Nucléaire et Corpusculaire (DNC-IN2P3/CNRS); Département Sciences de l’Univers (SDU-INSU/CNRS); Institut Lagrange de Paris (ILP) Grant No. LABEX ANR-10-LABX-63 within the Investissements d’Avenir Programme Grant No. ANR-11-IDEX-0004-02; Germany – Bundesministerium für Bildung und Forschung (BMBF); Deutsche Forschungsgemeinschaft (DFG); Finanzministerium Baden-Württemberg; Helmholtz Alliance for Astroparticle Physics (HAP); Helmholtz-Gemeinschaft Deutscher Forschungszentren (HGF); Ministerium für Kultur und Wissenschaft des Landes Nordrhein-Westfalen; Ministerium für Wissenschaft, Forschung und Kunst des Landes Baden-Württemberg; Italy – Istituto Nazionale di Fisica Nucleare (INFN); Istituto Nazionale di Astrofisica (INAF); Ministero dell’Università e della Ricerca (MUR); CETEMPS Center of Excellence; Ministero degli Affari Esteri (MAE), ICSC Centro Nazionale di Ricerca in High Performance Computing, Big Data and Quantum Computing, funded by European Union NextGenerationEU, reference code CN_00000013; México – Consejo Nacional de Ciencia y Tecnología (CONACYT) No. 167733; Universidad Nacional Autónoma de México (UNAM); PAPIIT DGAPA-UNAM; The Netherlands – Ministry of Education, Culture and Science; Netherlands Organisation for Scientific Research (NWO); Dutch national e-infrastructure with the support of SURF Cooperative; Poland – Ministry of Education and Science, grants No. DIR/WK/2018/11 and 2022/WK/12; National Science Centre, grants No. 2016/22/M/ST9/00198, 2016/23/B/ST9/01635, 2020/39/B/ST9/01398, and 2022/45/B/ST9/02163; Portugal – Portuguese national funds and FEDER funds within Programa Operacional Factores de Competitividade through Fundação para a Ciência e a Tecnologia (COMPETE); Romania – Ministry of Research, Innovation and Digitization,

CNCS-UEFISCDI, contract no. 30N/2023 under Romanian National Core Program LAPLAS VII, grant no. PN 23 21 01 02 and project number PN-III-P1-1.1-TE-2021-0924/TE57/2022, within PNCDI III; Slovenia – Slovenian Research Agency, grants P1-0031, P1-0385, I0-0033, N1-0111; Spain – Ministerio de Ciencia e Innovación/Agencia Estatal de Investigación (PID2019-105544GB-I00, PID2022-140510NB-I00 and RYC2019-027017-I), Xunta de Galicia (CIGUS Network of Research Centers, Consolidación 2021 GRC GI-2033, ED431C-2021/22 and ED431F-2022/15), Junta de Andalucía (SOMM17/6104/UGR and P18-FR-4314), and the European Union (Marie Skłodowska-Curie 101065027 and ERDF); USA – Department of Energy, Contracts No. DE-AC02-07CH11359, No. DE-FR02-04ER41300, No. DE-FG02-99ER41107 and No. DE-SC0011689; National Science Foundation, Grant No. 0450696, and NSF-2013199; The Grainger Foundation; Marie Curie-IRSES/EPLANET; European Particle Physics Latin American Network; and UNESCO.